HIGH PRECISION ^{26}Al-^{26}Mg ISOTOPE SYSTEMATICS FOR AN ALMOST PRISTINE REFRACTORY INCLUSION: IMPLICATIONS FOR THE ABSOLUTE AGE OF THE SOLAR SYSTEM.

M. Wadhwa[1] N. T. Kita[2], D. Nakashima[2], E. S. Bullock[3], G. J. MacPherson[4], and A. Bouvier[5], [1]Center for Meteorite Studies, School of Earth and Space Exploration, Arizona State University, Tempe, AZ 85287 (wadhwa@asu.edu), [2]WiscSIMS, Department of Geoscience, University of Wisconsin-Madison, Madison, WI 53706, [3]Department of Mineral Sciences, National Museum of Natural History, Smithsonian Institution, Washington, DC 20560, [4]Department of Earth Sciences, University of Western Ontario, London, ON, Canada N6A 5B7.

Introduction: Calcium-aluminum-rich inclusions (CAIs) found in primitive chondrites represent the earliest solids to have formed in the early Solar System. ([1] and references therein). As such, these objects can be considered to be markers that define the beginning of the Solar System (T_0) and provide a record of the earliest epoch in the evolution of the Solar protoplanetary disk. Since the recognition of ^{238}U/^{235}U variations in calcium-aluminum-rich inclusions (CAIs) [2], only a few studies have been conducted where Pb-Pb ages were reported for CAIs for which the U isotope compositions were also measured [3-5]. These ages range from 4567.2±0.5 Ma and 4567.3±0.2 Ma for CAIs from Allende [3] and Efremovka [5], respectively, to 4567.9±0.3 Ma for a CAI from Northwest Africa (NWA) 6991 [4]. Previous studies have shown that both the Allende and Efremovka parent bodies experienced significant but variable alteration [6,7] and thus CAIs in these CV meteorites may have been affected to varying degrees. This raises the possibility that the systematically younger ages of CAIs in these meteorites may be the result of isotopic disturbance, and that CAIs in other, potentially less altered, primitive chondrites should be investigated for determining the chronology of Solar System formation. The CV3 chondrite NWA 6991, which records a low shock stage and shows minimal terrestrial weathering, may be such a sample [8].

We recently reported preliminary in situ laser ablation MC-ICPMS Al-Mg analyses of a CAI from NWA 6991 (known as "B4"), which yielded a near-canonical ^{26}Al/^{27}Al of (5.5 ± 0.3) × 10^{-5}. Here we report further high-precision, high spatial resolution Al-Mg systematics determine by multicollector ion microprobe which demonstrate that this CAI may be one of the most pristine objects studied thus far.

Analytical Techniques: A polished thin section containing two slices of the NWA 6991 B4 CAI was characterized using the FEI NOVA NanoSEM 600 scanning electron microscope (SEM) and JEOL 8900 electron microprobe at the Smithsonian Institution. The Al-Mg isotopic analyses were performed using a Cameca IMS-1280 secondary ion mass spectrometer (SIMS) at the University of Wisconsin (UW) using protocols similar to those described previously [9]. Additional SEM images were obtained using a Hitachi S3400-N at UW before and after the SIMS analyses. The Mg-poor anorthite was analyzed using a ~10 μm beam spot (0.8 nA intensity) and a single electron multiplier in peak-switching mode. Magnesium isotopes in melilite, spinel and pyroxene were analyzed with multicollector faraday detectors using intense primary beam conditions (23 nA with beam size of 40 μm for melilite; 12 nA with a beam size of 25 μm for spinel and pyroxene). ^{27}Al signals were collected on a faraday detector simultaneously with Mg isotopes in all cases. Both natural and instrumental mass fractionation were corrected using an exponential law with β=0.514. Radiogenic excesses in the ^{26}Mg/^{24}Mg ratio are reported as per mil deviations relative to terrestrial standards (δ^{26}Mg*).

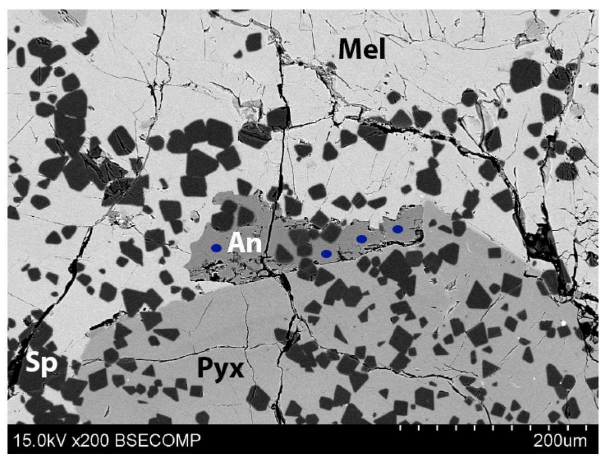

Figure 1. BSE image of a representative area of the B4 CAI showing the main phases (An = anorthite; Pyx = pyroxene; Mel: melilite; Sp = spinel) comprising this inclusion. Blue symbols show the size and location of the ion microprobe spots on an anorthite grain that was analyzed in this area.

Results and Discussion: The B4 CAI from NWA 6991 is a coarse-grained Compact Type (CTA) inclusion composed mainly of melilite, spinel, pyroxene, and anorthite. The mineralogic and petrographic features of this inclusion are discussed in more detail in a companion abstract [10].

Figure 1 shows a representative area of this inclusion that was analyzed with the ion microprobe. In all, 56 spot analyses were conducted (32 on melilite, 7 on spinel, 9 on pyroxene and 8 on anorthite). Anorthite is the phase with the highest $^{27}Al/^{24}Mg$ ratios ranging from ~211 to ~543. Melilite shows a substantial range in $^{27}Al/^{24}Mg$ ratios, from ~1 to ~39. Pyroxene has a relatively narrow range ($^{27}Al/^{24}Mg$ ~1.8-2.8) while spinel has uniform $^{27}Al/^{24}Mg$ of ~2.56, consistent with stoichiometric $MgAl_2O_4$ [10]. All the data taken together define an isochron with a slope corresponding to an initial $^{26}Al/^{27}Al$ of (4.90 ± 0.05) × 10^{-5} and an initial $\delta^{26}Mg^*$ ($\delta^{26}Mg^*_0$) of 0.15 ± 0.13 ‰, which includes uncertainties in the SIMS relative sensitivity factors used to calculate the $^{27}Al/^{24}Mg$ ratios. The MSWD (=1.5) for the fit to this isochron is significantly smaller than that for internal Al-Mg isochrons obtained for other coarse-grained melted (CTA or Type B) CAIs previously analyzed using SIMS [9, 11].

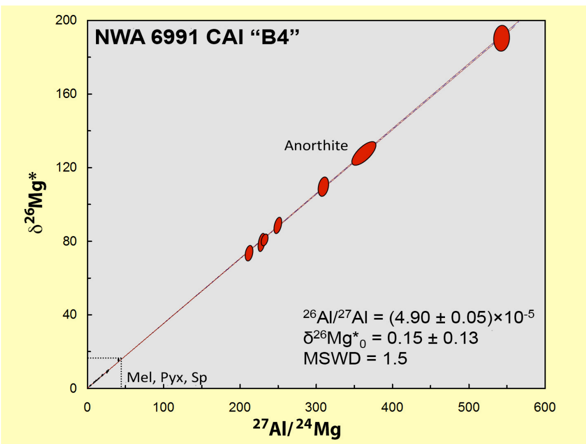

Figure 3. The ^{26}Al-^{26}Mg isochron defined by all 56 data points obtained on anorthite, melilite, pyroxene and spinel of the NWA 6991 CAI B4. The box on the lower left is shown in more detail in Fig. 4 below.

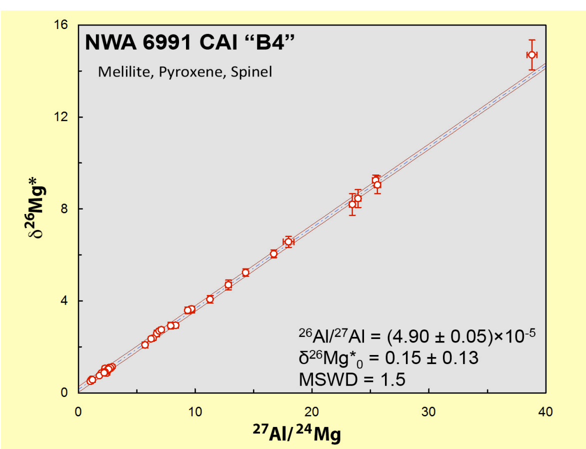

Figure 4. A detailed view of the lower left region of the isochron diagram shown in Fig. 3, showing only the melilite, pyroxene and spinel data.

As can be seen in Figs. 3 and 4, all of the data points, with one exception, lie on a single best-fit line regressed through all the data. A single melilite data point (with the highest Al/Mg ratio of ~39) lies slightly above this best-fit line. This analysis point was noted to lie close to the rim of the inclusion, and it is possible that there is minor disturbance of the Al-Mg system in this region owing to a small degree of equilibration with the matrix. If this melilite data is excluded from the regression, this yields an initial $^{26}Al/^{27}Al$ of (4.90 ± 0.05) × 10^{-5} and $\delta^{26}Mg^*_0$ of 0.13 ± 0.12 ‰ (MSWD = 1.5), essentially similar to the values obtained when all the data are included.

The petrology [10] and internal Al-Mg systematics of this CAI suggest that it is undisturbed by secondary alteration processes (such as metamorphism or hydrous alteration), and is perhaps the most pristine CAI for which internal Al-Mg systematics have been obtained so far. Its initial $^{26}Al/^{27}Al$ and $\delta^{26}Mg^*_0$ are in the range of values obtained from internal isochrons of melted CTA or Type B CAIs from other chondrites such as Allende, Leoville and Vigarano [9,11-15]. This initial $^{26}Al/^{27}Al$ is slightly lower than the canonical ratio of ~5.25 × 10^{-5} (and the $\delta^{26}Mg^*_0$ is slightly higher than) obtained from bulk CAI isochrons and from internal isochrons for fine-grained, unmelted CAIs [11-13,16]. This is consistent with the time scales and sequence of initial condensation and subsequent heating/melting of fine-grained and coarse-grained inclusions, respectively, [11] and suggests that the thermal processing of B4 occurred within at most ~0.08 Ma after the formation of unmelted, fine-grained CAIs. This time interval is well within the precision that is currently possible for the Pb-Pb age calculations when error in the U isotopic measurements is also included (~±0.2-0.3 Ma). As such, the Pb-Pb age recently reported for the NWA 6991 B4 CAI of 4567.9 ± 0.3 Ma [4] is likely to be a good approximation of T_0 for our Solar System.

References: [1] MacPherson G. J. (2014) *Treatise on Geochem.* (2nd Ed.), *1,* 139-179. [2] Brennecka G. et al. (2010) *Science,* 327, 449-451. [3] Amelin Y. et al. (2010) *EPSL, 300,* 343-350. [4] Bouvier A. et al. (2011) *Workshop on Formation of the First Solar System Solids*, Abstract #9054. [5] Connelly J. N. et al. (2012) *Science, 338,* 651-655. [6] Scott E. R. D. et al. (1992) *GCA, 56,* 4281-4293. [7] Krot A. N. et al. (1995) *MAPS, 30,* 530-531. [8] Meteoritical Bulletin 100, *MAPS, 46*. [9] Kita N. T. et al. (2012) *GCA, 86,* 37-51. [10] Bullock E. S. et al. (2014) *this meeting*. [11] MacPherson G. J. et al. (2012) *EPSL, 331-332,* 43-54. [12] Kita N. T. et al. (2013) *MAPS, 48,* 1383-1400. [13] Jacobsen B. et al. (2008) *EPSL, 272,* 353-364. [14] Bouvier A. And Wadhwa M. (2010) *Nature Geosci., 3,* 637-641. [15] MacPherson G. J. et al. (2010) *ApJ., 711,* L117-L121. [16] Thrane K. et al. (2006) *ApJ., 646,* L159-L162.